Article Information

Journal Title: Journal of materials synthesis and processing

7347

Volume: 1   **Issue:** 1
Month/Year: 1993   **Pages:** 43-43
Article Author: R Fedou, F Langlais, R Naslain

Article Title: Model for the isothermal isobaric chemical vapor infiltration in a straight cylindrical pore. 1. Description of the model

Loan Information

Loan Title:

Loan Author:

Publisher:
Place:
Date:
Imprint:

Borrower Information

NEW: Main Library

Odyssey: 206.107.45.51
Email:
NOTES
/
2/28/2023

A Model for the Isothermal Isobaric Chemical Vapor Infiltration in a Straight Cylindrical Pore. 1. Description of the Model

R. Fédou,[1] F. Langlais,[1,2] and R. Naslain[1]

Chemical vapor infiltration is a convenient method for elaborating ceramic matrix composites by densifying porous preforms made of ceramic fibers. In order to predict the densification rate and infiltration homogeneity, a numerical model is proposed concerning (i) a straight, cylindrical open-ended pore with a large aspect ratio and (ii) any chemical system, including the solid deposit and the gaseous phase (reactant species, product species, and carrier gas), defined by the stoichiometry and the kinetics of the heterogeneous reaction. Three kinds of equations are considered in this one-dimensional model: (i) the equations of mass transfer for each gaseous species, based on Fick and Knudsen diffusion and a convection term resulting from the gaseous mole number changes in the deposition reaction; (ii) the boundary conditions at the entrances and the center of the pore; and (iii) the equation for the local change of pore geometry. To solve the various equations, a finite-differences method is used, which permits calculation—at any stage of the densification, and particularly at the end of the process, when the pore is closed—of the concentration profiles of each gaseous species and the diameter profile. A first validation of the model is given by comparing its results with those obtained from previous models.

KEY WORDS: Chemical vapor infiltration; straight cylindrical pore; numerical model; ceramic matrix composites.

1. INTRODUCTION

Chemical vapor infiltration (CVI) is a very convenient technique for the processing of ceramic matrix composites (CMC). These materials are prepared by densifying refractory fibrous preforms (usually made of carbon, silicon carbide, or alumina fibers) with a deposit resulting from a heterogeneous gas–solid chemical reaction taking place on the internal surface of the pore network of the preform. This technique was successfully applied to various refractory matrices such as pyrocarbon, carbides (SiC, TiC, B_4C), nitride (BN), and oxides (Al_2O_3, ZrO_2) [1–9].

In the classical isothermal isobaric technique (ICVI), infiltration temperature and pressure must be chosen in order to favor in-depth deposition with respect to external surface coating. These conditions result in decreasing the residual porosity of the composites so prepared but also in raising the densification durations. In spite of these drawbacks, the ICVI is suitable for densifying simultaneously a large number of preforms with complex and various shapes, without damaging the ceramic fibers.

With a view to accelerating the infiltration process, the use of a gradient of pressure and/or temperature through the preform has been studied. But these techniques of forced CVI (FCVI) require specific tools and are not very flexible [10]. The choice of convenient infiltration conditions, even in the case of the widely studied SiC and pyrocarbon matrices, is still empirical owing to the complexity of the actual porous substrates and

[1] Laboratoire des Composites Thermostructuraux, UMR 47 CNRS-SEP-UB1, Domaine Universitaire, 3 Allée La Boétie, 33600 Pessac, France.
[2] To whom correspondence should be addressed.

the physical and chemical phenomena. A thorough study of the infiltration mechanisms, resulting in previsional models, seemed necessary in order to optimize both the homogeneity of CVI-processed composites and the densification rates. These models need simplified geometric descriptions which simulate the actual fibrous preforms. These equivalent porous media are not yet available. So the first model which will permit an understanding of the mechanisms involved can be constructed for the case of a single straight cylindrical pore. This kind of geometry has already been selected in a few recently published studies [4, 11–19].

Most recent papers in this field are based on old works carried out by Thiele in the field of theoretical studies on the efficiency of porous catalysts [11]. That author built a one-dimensional (1D) model taking into account the diffusive transfers and the chemical reaction occurring in a straight cylindrical pore with a constant diameter. The analytical solution of mass balance equations in the steady state resulted, for first-order kinetics with respect to the reactant species, in concentration profiles and effective reaction rates as a function of a dimensionless number (proportional to the ratio between the kinetic constant of the heterogeneous reaction and the diffusion coefficient) presently referred to as the Thiele modulus. The same kind of approach was used by Petersen for etching chemical reactions, such as gasification of graphite by CO_2. The proposed model permitted prediction of the increase in radius of a cylindrical pore [12]. This author validated the quasi-steady-state hypothesis, which requires that the mass transfers be very rapid with respect to the variations of the pore geometry.

In the field of CVI modeling itself, Fitzer and Gadow calculated, for the first time, theoretical infiltration depths on the basis of limit values of the Thiele modulus by assuming, as in catalysts, that the infiltration efficiency is given by the ratio between the deposition rate within the pore and the deposition rate at the pore entrance [13]. Van den Brekel et al. proposed a 2D analytical modeling of the CVD process in a macroscopic cylindrical tube whose radius was assumed not to depend on time [14]. They considered, on the one hand, chemical reactions with orders close to one and, on the other hand, transfers occurring only by Fick diffusion. For first-order kinetics, they found exactly the analytical solution of the 1D model proposed by Thiele. Then Rossignol et al. applied this model to CVI in a microscopic cylinder [4]. They introduced Knudsen diffusion and assumed a reaction order equal to one and a cylindrical geometry of the pore with a time-dependent di-

ameter. Similar models, applied to the infiltration of various ceramics (SiC and Al_2O_3 for composites, ZrO_2 (Y_2O_3) for porous membranes [15]), dealt with 1D or quasi-1D calculations, under the hypothesis of the quasi-steady state, taking into account Knudsen diffusion transfers.

A few authors introduced, in the equations of mass conservation, a convection term originating from either a gaseous mole number variation related to the heterogeneous reaction [11, 15] or a forced flow in the porous substrate [20]. In most studies, only the heterogeneous reactions are considered and assumed to be first order with respect to the precursor species [16–18, 20]. Conversely, Lin et al. showed in their model the influence of reaction orders ranging between 0 and 2 on the deposition profiles [15]. Recently, Middleman proposed an analytical model including, besides the heterogeneous reaction, a homogeneous reaction resulting in the formation of an intermediate species [18].

In most of the previously mentioned models, the effects of the pore geometry variations during the infiltration process were sometimes discussed but usually they were not taken into account in the calculations. Nevertheless, the Knudsen diffusion coefficient and, consequently, the Thiele modulus depend on the pore radius, which varies as a function of both time and spatial coordinate along the pore. The aim of the present article is to describe in some detail a model which predicts gaseous species concentration profiles and diameter profiles and which includes (i) the local pore geometry, (ii) multicomponent chemical systems, (iii) any heterogeneous kinetics, and (iv) the gaseous precursor, not necessarily diluted. The use of this model in the case of several chemical systems (CVI of SiC and oxides such as ZrO_2 and Y_2O_3), with a few experimental comparisons, is proposed in two subsequent papers (Parts 2 and 3 [21, 22]).

2. DESCRIPTION OF THE MODEL

2.1. Geometry of the Pore

The pore considered here is a straight cylindrical open-ended pore with an initial diameter Φ_0 and a length L (Fig. 1). The boundary conditions are identical at both ends, i.e., the pore is symmetrical with respect to its center, and the study is thus limited to one half of the pore. Due to the symmetry with respect to its axes, the pore is assumed to remain straight during the infiltration process, and any cross section is a disk.
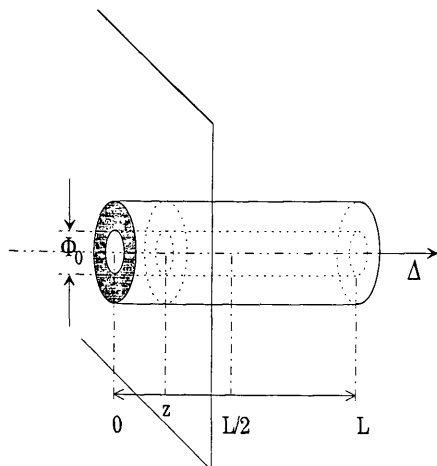
Fig. 1. Geometrical features of the straight cylindrical model pore.

2.2. Hypotheses

(1) The temperature is supposed to be constant not only versus time, but also in the whole pore volume (isothermal process).

(2) No homogeneous reaction occurs within the pore.

(3) The mass transfers within the pores are controlled only by diffusion processes, the forced convection phenomena being negligible in small pores. Nevertheless, the convection terms, which result from the mole number changes in the chemical reactions, are considered but can become zero when the reactive species are highly diluted.

(4) The mass transfers are assumed to be very rapid with respect to the rate of variation of the pore geometry, i.e., the infiltration can be considered as a series of quasi-steady states. This assumption is analytically justified by Petersen in his study of the gasification of graphite [12] and by Gupte and Tsamopoulos, who found mass transfers at least 100 times more rapid than the variations of the pore geometry [16].

(5) The concentrations of the gaseous species are constant in a cross section of the pore, i.e., the radial diffusional fluxes are negligible compared to the axial fluxes, which permits the reduction of a 2D problem to a 1D problem. This hypothesis can be justified by (i) a large aspect ratio (L/Φ_0), (ii) the identical analytical results obtained by Van den Brekel with a 2D model [14] and Thiele with a 1D model [11], and (iii) the homogeneity of deposit thickness observed experimentally in straight pores with a rectangular cross section of a straight pore [23].

2.3. Space and Time Variables

The axial coordinate, z, is defined as the distance from the nearest pore entrance (i.e., $0 \leq z \leq L/2$). The reduced infiltration depth is the adimensional variable $z' = z/L$.

The time origin ($t = 0$) is chosen to correspond to the first mass transfer steady state, which is assumed to be set up very rapidly compared to the rate of variations of the pore diameter. The time needed to close the pore is called t_c. An adimensional time is also defined as $t' = t/t_c$.

The geometry of the pore at time t is totally described by the function $\Phi(z, t)$, which gives the diameter of the pore for any value of z.

2.4. The Chemical System

The chemical system involved in the heterogeneous reaction of the CVI process can be described as a set of species: a solid phase produced on the pore walls and a gaseous phase including three kinds of species—(i) those consumed at the solid surface, (ii) those produced by the deposition reaction, and possibly (iii) inert species used as a carrier gas such as Ar.

Generally speaking, the heterogeneous chemical reaction can be written as

$$\sum_1 \nu_1 A_1 = 0 \tag{1}$$

where A_1 represents the gaseous or solid chemical species 1 and ν_1 is the stoichiometric coefficient related to species 1 (which is positive for the reaction products, negative for the reactants, and nil for the inert species).

For a given reaction, Eq. (1) can be written so that the stoichiometric coefficient is 1 for the deposited solid.

According to these conditions and using the concept of the extent of reaction ξ (mol) [24], the rate of the heterogeneous reaction for the production of 1 mol of solid on a unit surface is defined as follows:

$$\vartheta = \frac{\partial^2 \xi}{\partial t \partial S} \tag{2}$$

where S is the area of the surface where the reaction occurs. ϑ can be expressed like a molar flux, as mol · m^{-2} s^{-1}. Consequently, the rate of consumption or production of the gaseous species i can be written as a molar flux to or from the reaction surface:

$$N_i = \frac{\partial (\nu_i \xi)}{\partial t \partial S} = \nu_i \vartheta \tag{3}$$

The reaction rate ϑ depends on the temperature, the total pressure, and the composition of the gaseous phase close to the deposition surface. Species with $\nu_i = 0$ can play an important kinetic role, i.e., as catalyst or inhibitor.

2.5. Equations of the Model

2.5.1. Mass Transfer Equations

The time variations of the concentration profiles for the various gaseous species and the deposit thickness profiles can be investigated by solving the mass balance equations for each species. The conservation equation for species i, resulting from the z component of the general vector equation of mass transfer in cylindrical coordinates (hypothesis 5), can be expressed in terms of molar units as follows [25]:

$$\frac{\partial C_i}{\partial t} + \frac{\partial N_i}{\partial z} = R_i \tag{4}$$

where C_i is the concentration of species i (mol $\cdot$ m^{-3}), N_i is the absolute molar flux of species i (mol $\cdot$ m^{-2} s^{-1}), and R_i is an algebraic term of source ($R_i > 0$) or sink ($R_i < 0$) for species i (mol $\cdot$ m^{-2} s^{-1}).

According to hypothesis 4 of the quasi-steady state, this equation is obviously simplified in

$$\frac{\partial N_i}{\partial z} = R_i \tag{5}$$

The term R_i can be deduced from a local treatment, by writing the conservation of the mole number of species i over a thin shell of pore (δz in thickness, $\mathcal{C}$ in section, and $\mathcal{P}$ in perimeter): The rate of consumption or production of species i by chemical reaction on the side wall of this shell must be equal to the difference between the algebraic flow rate of i through the cross section at $z + \delta z$, i.e.,

$$\nu_i \vartheta \mathcal{P} \Delta z = [N_i(z) - N_i(z + \Delta z)]\mathcal{C} \tag{6}$$

By taking the limit as δz approaches zero, we obtain:

$$\frac{\partial N_i}{\partial z} = \frac{\nu_i \vartheta \mathcal{P}}{\mathcal{C}} \tag{7}$$

In the particular case of a cylindrical pore, Eq. (7) is equal to:

$$\frac{\partial N_i}{\partial z} = \frac{4\nu_i \vartheta}{\Phi} \tag{8}$$

If this equation is summed on all the gaseous species i, it becomes

$$\frac{\partial N}{\partial z} = \frac{4\Delta\nu\vartheta}{\Phi} \tag{9}$$

with

$$N = \sum_{i=1}^{n_g} N_i \tag{10}$$

and

$$\Delta\nu = \sum_{i=1}^{n_g} \nu_i \tag{11}$$

where N is the total gaseous molar flux and $\Delta\nu$ is the overall variation of the gaseous mole number resulting from the heterogeneous reaction.

According to hypothesis 3, the absolute molar flux includes a pure diffusion term (i.e., first Fick law) and a convective term (which is positive if the heterogeneous reaction consumes gaseous molecules and negative in the opposite case), usually called the Stefan flow:

$$N_i = -D_i \frac{\partial C_i}{\partial z} + x_i N \tag{12}$$

where D_i is the diffusion coefficient of species i in the gaseous mixture (m^2 s^{-1}) and x_i is the molar fraction of species i, defined by

$$x_i = \frac{C_i}{\sum_{j=1}^{n_g} C_j} \tag{13}$$

By combining Eqs. (8) and (12) and neglecting the term including the derivative of the diffusion coefficient, the mass transfer equation to be solved results as follows:

$$D_i \frac{\partial^2 C_i}{\partial z^2} - \frac{\partial(x_i N)}{\partial z} + \frac{4\nu_i \vartheta}{\Phi} = 0 \tag{14}$$

2.5.2. Diffusion Coefficient of Species i in the Gaseous Mixture

Classically, the mass transport phenomena by Fick diffusion are controlled by the collision of molecules. In the case of CVI, where diffusion occurs at high temperatures and low pressures in pores with low diameters, the mean free path of the molecules can be high with respect to the pore diameter, so the diffusion transport can be governed by the collision of the molecules on the walls: the Knudsen diffusion regime [26, 27]. Nevertheless, both mechanisms can occur in the CVI process

and an overall diffusion coefficient must be taken into account, according to the Bosanquet definition [27]:

$$\frac{1}{D_i} = \frac{1}{D_{i,\mathrm{F}}} + \frac{1}{D_{i,\mathrm{K}}} \quad (15)$$

where $D_{i,\mathrm{K}}$ is the Knudsen diffusion coefficient of species $i \,(\mathrm{m^2\ s^{-1}})$ and $D_{i,\mathrm{F}}$ is the Fick diffusion coefficient of species i in the gaseous mixture.

The coefficient $D_{i,\mathrm{F}}$ depends on the gaseous phase composition. Assuming that species i diffuses through a stagnant mixture, $D_{i,\mathrm{F}}$ can be calculated by the expression

$$\frac{1 - x_i}{D_{i,\mathrm{F}}} = \sum_{\substack{j=1 \\ j \langle \rangle i}}^{n_{\mathrm{g}}} \frac{x_j}{D_{i,j}} \quad (16)$$

where $D_{i,j}$ is the Fick diffusion coefficient for the binary gaseous mixture of species i and j. Every value of $D_{i,j}$ and, consequently, the value of $D_{i,\mathrm{F}}$ are proportional to $1/P$ and $T^{\beta}\,(1.2 \le \beta \le 2)$, P and T being the total pressure and the temperature of the CVI process (cf. Appendix 1).

Conversely the Knudsen diffusion coefficient depends only on the temperature and the geometry of the pore according to [26]

$$D_{i,\mathrm{K}} = \frac{\Phi}{3}\left[\frac{8\mathbf{R}T}{\pi M_i}\right]^{1/2} \quad (17)$$

where $\mathbf{R}$ is the ideal gas constant $(8.32\ \mathrm{J \cdot K^{-1}\ mol^{-1}})$ and M_i is the molar mass of species $i\ (\mathrm{kg \cdot mol^{-1}})$.

2.5.3. Boundary Conditions

At the pore entrance, the concentration C_i is assumed to be constant and set by the phenomena occurring outside the pore:

$$C_i(0, t) = C_{i,0} \quad (18)$$

At the center of the pore, the symmetry involves

$$\left[\frac{\partial C_i}{\partial z}\right]_{z = L/2} = 0 \quad (19)$$

and

$$(\mathbf{N})_{z = L/2} = 0 \quad (20)$$

2.5.4. Equation for the Pore Geometry Change

The coefficient $D_{i,\mathrm{K}}$ and the chemical reaction term of the mass transfer equation (14) being dependent on the pore diameter, another differential equation must be solved, which gives the diameter variations versus time

for position z (cf. Appendix 2):

$$\frac{\partial \Phi}{\partial t} = -2V_{\mathrm{s}}\vartheta \quad (21)$$

where V_{s} is the molar volume of the deposited solid $(\mathrm{m^3\ mol^{-1}})$.

3. SOLUTION METHOD

In order to solve the various partial differential equations which describe the system, it is necessary to use a numerical model which makes (i) the space and time and (ii) the equations discrete. For the differential equations, the finite-differences method [28] is used. This procedure is detailed in Appendix 3.

The general calculation procedure can be described as the following loop (Fig. 2).

(1) The geometry of the pore being fixed at time t_u, the concentration profiles are calculated for each gaseous species at time t_{u+1} by solving the system of Eqs. (A12), (A13), and (A15)–(A17) (Appendix 3).

(2) If these concentration profiles are put into Eq. (A18), the pore diameter profile can be calculated at time t_{u+1}.

(3) As the diameter of the pore influences the chemical source or sink term and the diffusion coefficient in Eqs. (A12) and (A15), the new concentration profiles at time t_{u+2} are then calculated as in step 1 by using the diameter profile at t_{u+1}.

The procedure begins with the cylindrical pore $(\Phi_{p,0} = \Phi_0)$, calculates concentration profiles and diameter profile as infiltration is going on, and is stopped
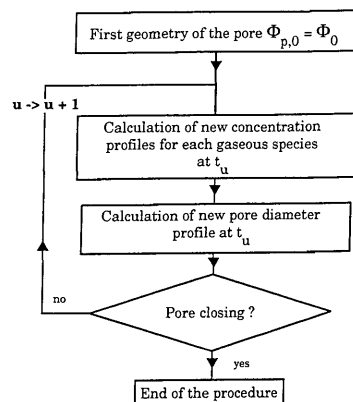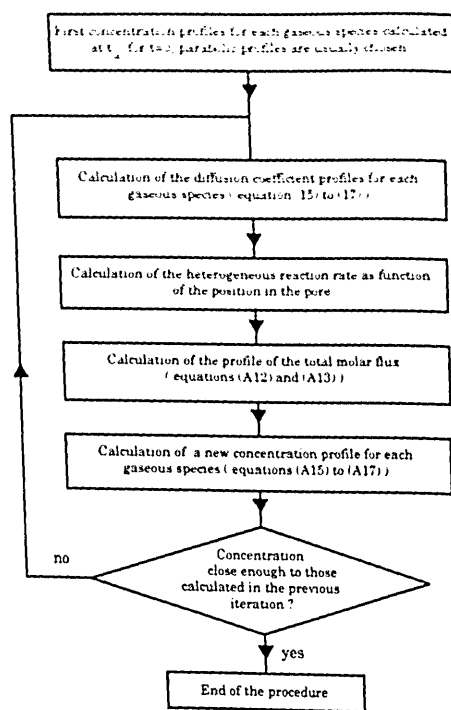

Fig. 2. General method of resolution.

Fig. 3. Calculation procedure of the concentration profiles for each gaseous species at time t_u.

when the pore is closed, usually at the entrances ($\Phi_p \leq 0$ for $p = 0$).

The step devoted to the calculation of the concentration profiles at time t_{u+1}, on the basis of the concentration profiles and diameter profile at t_u, uses an iterative method as shown in Fig. 3. For each iteration, the calculated profiles are different from those obtained in the previous step but are considered to be better until the difference between two successive calculations is lower than a given relative difference. The procedure is stopped when the convergence criterion is verified for all concentration profiles, and the last ones are assumed to be the most convenient.

The computation program for these various procedures is written in FORTRAN [29].

4. DATA ON THE CHEMICAL DEPOSITION PROCESS

4.1. Molar Volume of the Deposited Solid Phase

If the solid deposited from the heterogeneous reaction is a pure phase without microporosity, its molar volume (m^3 mol^{-1}) is given by

$$V_s = \frac{M_s}{\rho_s} \tag{22}$$

where M_s is the molar mass of the deposited phase ($kg \cdot mol^{-1}$) and ρ is the specific mass of the deposited phase ($kg \cdot m^{-3}$).

If the chemically deposited solid is made of n_s phases, the corresponding molar volume (i.e., for an extent of reaction of 1 mol) can be written as

$$V_s = \frac{1}{\sum\limits_{w=1}^{n_s} \nu_w} \sum_{v=1}^{n_s} \nu_v \frac{M_v}{\rho_v} \tag{23}$$

where ν_v is the stoichiometric coefficient of the solid phase v in the heterogeneous reaction (as defined in Section 2.4), M_v is the molar mass of the solid phase v ($kg \cdot mol^{-1}$), and ρ_v is the specific mass of the solid phase v ($kg \cdot m^{-3}$).

4.2. Heterogeneous Reaction Rate

In the equation of mass transfer (13), the term ϑ is the rate of production of solid phase per unit area. This term is a function of the temperature, the total pressure, and the composition of the gaseous phase near the deposition surface. This function, i.e., the kinetic law, can be derived from experiments on flat substrates. These experiments yield (i) the domain where the kinetics is controlled by the chemical reactions, (ii) the activation energies by drawing Arrhenius plots, and (iii) reaction orders with respect to reactant and product species. The main problem in CVI is to express the kinetic laws as a function of the intermediate species which result from homogeneous reactions occurring in the hot zone and which actually react at the solid surface (e.g., the pore wall).

For a first-order kinetic law for a single precursor species I with an initial concentration C_I^0 ($mol \cdot m^{-3}$), the deposition rate ϑ ($mol \cdot m^{-2}$ s^{-1}) can be expressed as

$$\vartheta = k_a C_I^0 \tag{24}$$

where k_a is the kinetic constant of the overall reaction ($m \cdot s^{-1}$).

In a hot-wall reactor, this precursor species I is very often decomposed into intermediates before reaching the reaction surface. If it is assumed that only one of these intermediates, species X, yields the solid deposit and its concentration C_X is proportional to C_I^0, then

$$C_X = k_h C_I^0 \tag{25}$$

where k_h is a constant related to the homogeneous reactions (dimensionless).

Combining Eqs. (24) and (25),

$$\vartheta = \frac{k_h}{k_a}, \qquad C_X = k_s C_X \qquad (26)$$

where $k_s(T)$ is the kinetic constant of the heterogeneous reaction ($m \cdot s^{-1}$).

For an infiltration process occurring in a cylindrical pore, the boundary conditions should take into account the gaseous phase composition at both ends of the pore, which results from the various homogeneous reactions. The quality of the densification depends on the kinetic constant of the heterogeneous reaction [e.g., $k_s(T)$]. So it is necessary to assess the local kinetic laws such as those given by Eq. (26).

5. VALIDATION OF THE MODEL

5.1. Comparison with the Van den Brekel Model

If the chemical system, including an inert species 1 and a species 2 which reacts into a solid phase, is considered under the following hypotheses—(i) no variation of the gaseous mole number in the deposition reaction ($\Delta\nu = 0$), (ii) first-order heterogeneous reaction with respect to species 2, and (iii) very high Knudsen diffusion coefficients of species 1 and 2 compared to the binary Fick diffusion coefficient—the model described previously can be reduced to a model very similar to those proposed by Thiele [11] and then by Van den Brekel et al. [14]. In this case, the terms containing the total molar flux can be removed [Eq. (9)] from mass transfer equations which are solved analytically and give the profile of species 2 along the pore:

$$\frac{C_2(z)}{C_2(0)} = \frac{\text{Cosh}\,[(1 - 2z/L)\tau]}{\text{Cosh}\,(\tau)} \qquad (27)$$

where

$$\tau = \sqrt{\frac{k_s L^2}{D_{1,2} \Phi_0}} \qquad (28)$$

is the Thiele modulus, with k_s ($m \cdot s^{-1}$) the kinetic constant of the heterogeneous reaction (from the first-order kinetic law $\vartheta = k_s C_2$) and $D_{1,2}$ ($m^2\,s^{-1}$) the Fick diffusion coefficient related to the binary mixture of species 1 and 2.

Equation (27) shows that the concentration within the pore is more homogeneous with a smaller Thiele modulus. By introducing identical data (i.e., values of L, Φ_0, k_s, $D_{1,2}$, and τ) in both the present and the Van den Brekel models, very similar results were obtained,

with relative differences lower than 10^{-3}. This validates the present model in a first simple case, which does not take into account the local variation of the diameter and the Knudsen diffusion.

5.2. Comparison with the Rossignol Model

The Rossignol model, derived from the Van den Brekel model, takes partially into account Knudsen diffusion and variations of the diameter but uses first-order kinetics and a binary gaseous mixture. A comparison between the present model and the Rossignol model can be made on the basis of thickness profiles calculated at the end of the infiltration process when the pore is closed (i.e., at $t = t_c$), in the case of the following chemical system: (i) a gaseous mixture of CH_3SiCl_3 (MTS)/H_2, (ii) a deposit of pure SiC with a density of 3.2, and (iii) first-order kinetics with respect to MTS (which is assumed not to react in the homogeneous phase), as follows:

$$\vartheta = k_0 \exp\left(-\frac{E_a}{RT}\right) C_{MTS} \qquad (29)$$

where k_0 is the frequency factor ($m \cdot s^{-1}$) and E_a is the activation energy of the reaction ($J \cdot mol^{-1}$).

The comparison is carried out for various values of the parameters T, P, Φ_0, and L. A few examples of these profiles calculated from both models are given in Fig. 4. Similar tendencies are observed when varying, e.g., the temperature, but a slight shift toward a less homogeneous infiltration is obtained for the Rossignol model. This shift can be attributed to the Rossignol hypothesis of a diameter equal to the entrance diameter (i.e., always lower than the actual diameter all along the pore), which results in an overestimated Thiele modulus and a worse infiltration profile [cf. Eqs. (27) and (28)].
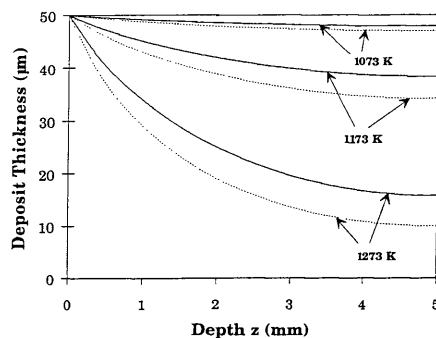

Fig. 4. SiC thickness profiles calculated from the present model (solid lines) and the Rossignol model (dashed lines) in a straight cylindrical half-pore for various temperatures and $P = 20$ kPa, $\Phi_0 = 100\ \mu m$, and $L/\Phi_0 = 100$.

APPENDIX 1: VALUATION OF FICK DIFFUSION COEFFICIENTS

Due to the difficulties in measuring the diffusion coefficients in the gases, particularly at high temperatures [30], valuation methods have been proposed by various authors.

The Hirschfelder Formula

In order to take into account attractive and repulsive forces between molecules, Hirschfelder $et\ al.$ performed various calculations on the Lennard–Jones potential leading to an expression of the Fick diffusion coefficients for a binary mixture between species i and species j [31]:

$$D_{i,j} = 5.876 \cdot 10^{-24} \frac{T^{3/2}}{P\sigma_{i,j}^2 \sqrt{}\Omega_D} \left[\frac{1}{M_i} + \frac{1}{M_j} \right]^{1/2} \quad (A1)$$

where $\sigma_{i,j}$ is the mean collision diameter (m), P is the total pressure (Pa), Ω_D is the Lennard–Jones collision integral (dimensionless), and M_i and M_j are the molar masses of species i and j (kg · mol^{-1}). Ω_D is a function of the adimensional factor $T^* = kT/\epsilon_{i,j}$, where k is the Boltzman constant and $\epsilon_{i,j}$ an energy term in the Lennard–Jones potential expression. Ω_D has been tabulated by Hirschfelder $et\ al.$ for various T^* values [32]. For intermediate values of T^*, linear interpolations are possible. As a consequence, it can be noted that $D_{i,j}$ does not depend exactly on $T^{3/2}$.

The Lennard–Jones constants $\sigma_{i,j}$ and $\epsilon_{i,j}$ for the binary mixture i, j can be determined from the characteristics of each species, according to

$$\sigma_{i,j} = \frac{\sigma_i + \sigma_j}{2} \quad (A2)$$

$$\frac{\epsilon_{i,j}}{k} = \left[\frac{\epsilon_i}{k} \cdot \frac{\epsilon_j}{k} \right]^{1/2} \quad (A3)$$

These individual constants can be found in tables or calculated with other formulas [25, 31]. When these various constants cannot be estimated, semiempirical expressions are used.

The Gilliland Formula

Gilliland proposed a semiempirical formula derived from the kinetic theory of gases, in order to estimate the Fick diffusion coefficient of a binary mixture i, j [33]:

$$D_{i,j} = 1.360 \cdot 10^{-3} \frac{T^{3/2}}{P(v_i^{1/3} + v_j^{1/3})^2} \left[\frac{1}{M_i} + \frac{1}{M_j} \right]^{1/2} \quad (A4)$$

where v_i and v_j are the molar volumes of species i and j at their boiling point (cm^3 mol^{-1}).

APPENDIX 2: DIFFERENTIAL EQUATION FOR THE PORE GEOMETRY CHANGE

The required equation results from a local treatment, by writing the volume of solid δV deposited on a thin shell of pore (δz in thickness) during time δt:

$$\delta V = \frac{\pi}{4} [\Phi^2(t) - \Phi^2(t + \delta t)] \delta z \quad (A5)$$

This volume can also be written as a function of the rate of the heterogeneous reaction ϑ and the molar volume of the deposited solid V_s:

$$\delta V = \vartheta \pi \Phi_t \delta z\, \delta t V_s \quad (A6)$$

Equation (A5) can be developed as follows:

$$\delta V = \frac{\pi}{4} \left\{ \Phi^2(t) - [\Phi(t) + \frac{\partial \Phi}{\partial t} \delta t]^2 \right\} \delta z \quad (A7)$$

or

$$\delta V = \frac{\pi}{4} \left\{ \Phi^2(t) - \Phi^2(t) - \left[\frac{\partial \Phi}{\partial t} \right]^2 \delta t^2 - 2\Phi(t) \frac{\partial \Phi}{\partial t} \delta t \right\} \delta z \quad (A8)$$

By combining Eqs. (A6) and (A8) [neglecting the second-order term in Eq. (A8)] with δt approaching zero, Eq. (21) is deduced:

$$\frac{\partial \Phi}{\partial t} = -2V_s \vartheta \quad (21)$$

APPENDIX 3: DISCRETIZATION PROCEDURE

Space Discretization

The half-pore is divided into n_z identical elements with a length

$$\Delta z = \frac{L}{2n_z} \quad (A9)$$

which results in a network made of $n_z + 1$ points located at the abscissa:

$$z_p = p\Delta z, \quad \text{with} \quad p = 0, 1, \cdots, n_z \quad \text{(A10)}$$

Time Discretization

Time t_c (as defined in Section 2.3) is divided into n_t identical periods with a duration

$$\Delta t = \frac{t_c}{n_t} \quad \text{(A11)}$$

which results in a network made of n_{t+1} instants t_u such as

$$t_u = u\Delta t, \quad \text{with} \quad u = 0, 1, \cdots, n_t$$

Discretization of the Partial Differential Equations

The functions occurring in the equations to be solved (e.g., the diameter of the pore and the concentrations of the gaseous species) are subjected to various indices as follows: first, i, j, k, and l for the chemical species; second, p for the space variable; and third, u for the time variable. For example, the concentration of species i at the abscissa z_p at the instant t_u is written $C_{i,p,u}$. Applying the finite-differences method, Eqs. (9) and (20), which allow us to calculate the profile of the total molar flux, and the mass transfer equation (14), discretized at the instant t_u, can be written as

$$\frac{N_{p+1} - N_p}{\Delta z} = \frac{4(\Delta v)_p \vartheta_p}{\Phi_p} \quad \text{(A12)}$$

with $0 \le p \le n_z - 1$,

$$N_{n_z} = 0 \quad \text{(A13)}$$

and

$$D_{i,p} \frac{C_{i,p+1} + C_{i,p-1} - 2C_{i,p}}{\Delta z^2}$$

$$- \frac{(x_i N)_{p+1} - (x_i N)_{p-1}}{2\Delta z} + \frac{4v_{i,p}\vartheta_p}{\Phi_p} = 0 \quad \text{(A14)}$$

with $1 \le p \le n_z - 1$.

Equation (A14) is equivalent to

$$-C_{i,p-1} + 2C_{i,p} - C_{i,p+1}$$

$$= \frac{4v_{i,p}\vartheta_p}{D_{i,p}\Phi_p} \Delta z^2 - \frac{(x_i N)_{p+1} - (x_i N)_{p-1}}{2D_{i,p}} \Delta z \quad \text{(A15)}$$

The boundary conditions on the concentrations [Eqs. (18) and (19)] become

$$C_{i,0,u} = C_{i,e} \quad \text{(A16)}$$

and

$$C_{i,n_z} = C_{i,n_z-1} \quad \text{(A17)}$$

Finally, discretizing between t_u and t_{u+1}, Eq. (21) for the diameter change leads to

$$\frac{\Phi_{p,u+1} - \Phi_{p,u}}{\Delta t} = -2(V_s)_p \vartheta_p \quad \text{(A18)}$$

with $1 \le p \le n_z$ and $0 \le u \le n_t - 1$.

ACKNOWLEDGMENTS

REFERENCES

1. F. Christin, R. Naslain, and C. Bernard, in *Proc. 7th Conf. CVD*, Los Angeles, CA, T. O. Sedgwick *et al.*, eds. (Electrochemical Society, Princeton, NJ, 1979), pp. 499–514.
2. E. Fitzer, D. Hagen, and J. Strohmeier, *Rev. Int. Hautes Temp. Refract.* **17**, 23 (1980).
3. H. Hannache, F. Langlais, and R. Naslain, in *Proc. 5th Eur. Conf. CVD*, Uppsala, Sweden, J. O. Carlsson *et al.*, eds. (Uppsala University Press, Uppsala, 1985), pp. 219–233.
4. J. Y. Rossignol, F. Langlais, and R. Naslain, in *Proc. 9th Int. Conf. CVD*, Cincinnati, OH, J. M. Blocher *et al.*, eds. (Electrochemical Society, Pennington, 1984), pp. 596–914.
5. H. Hannache, R. Naslain, and C. Bernard, *J. Less-Common Met.* **95**, 221 (1983).
6. R. Colmet, L. Lhermitte-Sebire, and R. Naslain, *Adv. Ceram. Mater.* **138**(2), 221 (1986).
7. R. Colmet *et al.*, *J. Electrochem. Soc.* **129**(6), 1367 (1982).
8. J. Minet, F. Langlais, and R. Naslain, *Compos. Sci. Technol.* **37**, 79 (1990).
9. J. Minet, F. Langlais, and R. Naslain, *J. Less-Common Met.* **132**, 273 (1987).
10. T. M. Bessmann *et al.*, in *Proc. 7th Eur. Conf. CVD*, Perpignan, France, M. Ducarroir *et al.*, eds. (Colloque de Physique, Les Editions de Physique, 1989), Colloque C5, Suppl. 5, Vol. 50, pp. 229–239.
11. E. W. Thiele, *Ind. Eng. Chem.* **31**(7), 916 (1939).
12. E. E. Petersen, *AIChE J.* **3**(4), 443–448 (1957).
13. E. Fitzer and R. Gadow, *Am. Ceram. Soc. Bull.* **65**, 326 (1986).
14. C. H. J. Van den Brekel *et al.*, in *Proc. 8th Int. Conf. CVD*, Paris, France, Mc D. Robinson *et al.*, eds. (Electrochemical Society, Pennington, 1984), pp. 142–156.
15. Y. S. Lin, K. J. De Vries, and A. J. Burggraaf, in *Proc. 7th Eur. Conf. CVD*, Perpignan, France, M. Ducarroir *et al.*, eds. (Colloque de Physique, Les Editions de Physique, 1989), Colloque C5, Suppl. 5, Vol. 50, pp. 861–872.

16. S. M. Gupte and J. A. Tsamopoulos, *J. Electrochem. Soc.* **136**(4), 555 (1989).

17. N. H. Tai and T. W. Chou, *J. Am. Ceram. Soc.* **72**(3), 414 (1989).

18. S. Middleman, *J. Mater. Res.* **4**(6), 1515 (1989).

19. M. F. Carolan and J. N. Michaels, *Solid State Ion.* **25**, 207 (1987).

20. T. L. Starr, in *Proceedings, International Conference on Wiskers-and-Fiber-Toughened Ceramics*, Oak Ridge, TN, R. A. Bradley *et al.*, eds. (ASM International, Oak Ridge, TN, 1988), pp. 243–252.

21. R. Fédou, F. Langlais, and R. Naslain, submitted for publication.

22. R. Fédou, F. Langlais, and R. Naslain, submitted for publication.

23. R. Fédou *et al.*, in press.

24. P. Molaës and J. C. Molaës, *Cinétique Chimique et Chimie Organique* (Vuibert, Paris, 1985).

25. R. B. Bird, W. E. Stewart, and E. N. Lightfoot, *Transport Phenomena* (J. Wiley and Sons, New York, 1960).

26. M. Knudsen, *The Kinetic Theory of Gases*, 3rd ed. (Wiley, New York, 1950).

27. P. C. Carman, *L'écoulement des gas à travers les milieux poreux*, J. Machefer, trans. (PUF, Paris, 1961).

28. M. Sibony and J.-Cl. Mardon, *Analyse Numérique II—Approximations et Equations Différentielles* (Hermann, Paris, 1988).

29. J. P. Lamoitier, *Le Langage FORTRAN IV* (Dunod Université, Paris, 1978).

30. J. Salvinien, B. Brun, and J. Apell, *Mesure des coefficients de diffusion, Séparation chimique* (Les Techniques de l'Ingénieur, Paris), p. 1515.

31. J. O. Hirschfelder, R. B. Bird, and E. L. Spotz, *Chem. Rev.* **44**, 205 (1949).

32. J. O. Hirschfelder, C. F. Curtis, and R. B. Bird, *Molecular Theory of Gases and Liquid* (Wiley, New York, 1954).

33. E. R. Gilliland, *Ind. Eng. Chem.* **26**, 681 (1934).